

# Geophysical Research Letters

## RESEARCH LETTER

10.1029/2020GL087921

### Key Points:

- Fluvial morphodynamic hierarchy can explain how common, rather than extreme, transport conditions are routinely preserved in strata
- The presence of morphodynamic hierarchy in a fluvial network increases the preservation of all lower-order hierarchical elements
- Preservation of a given morphodynamic level is highest when its evolution timescale is comparable to that of the next highest level

### Supporting Information:

- Supporting Information S1

### Correspondence to:

V. Ganti,  
vganti@ucsb.edu

### Citation:

Ganti, V., Hajek, E. A., Leary, K., Straub, K. M., & Paola, C. (2020). Morphodynamic hierarchy and the fabric of the sedimentary record. *Geophysical Research Letters*, *47*, e2020GL087921. <https://doi.org/10.1029/2020GL087921>

Received 13 MAR 2020

Accepted 1 JUN 2020

Accepted article online 9 JUN 2020

## Morphodynamic Hierarchy and the Fabric of the Sedimentary Record

Vamsi Ganti<sup>1,2</sup> , Elizabeth A. Hajek<sup>3</sup> , Kate Leary<sup>1</sup> , Kyle M. Straub<sup>4</sup> , and Chris Paola<sup>5</sup> 

<sup>1</sup>Department of Geography, University of California, Santa Barbara, CA, USA, <sup>2</sup>Department of Earth Science, University of California, Santa Barbara, CA, USA, <sup>3</sup>Department of Geological Sciences, Pennsylvania State University, State College, PA, USA, <sup>4</sup>Department of Earth and Environmental Sciences, Tulane University of Louisiana, New Orleans, LA, USA, <sup>5</sup>Department of Earth Science and St. Anthony Falls Laboratory, University of Minnesota, Twin Cities, Minneapolis, MN, USA

**Abstract** The low temporal completeness of fluvial strata could indicate that recorded events represent unusual and extreme conditions. However, field observations suggest that preserved strata predominantly record relatively common transport conditions—a paradox termed the *strange ordinarieness* of fluvial strata. We theorize that the self-organization of fluvial systems into a morphodynamic hierarchy that spans bed to basin scales facilitates the preservation of ordinary events in fluvial strata. Using a new probabilistic model and existing field and experimental data sets across these scales, we show that fluvial morphodynamic hierarchy enhances the stratigraphic preservation of medial topography—ordinary events. We show that lower-order landforms have a higher likelihood of complete preservation when the kinematic rates of evolution of successive levels in the morphodynamic hierarchy are comparable. We highlight how relative changes in kinematic rates of evolution of successive levels in the morphodynamic hierarchy can manifest as major shifts in stratigraphic architecture through Earth history.

**Plain Language Summary** Earth's ability to archive its evolution in sedimentary rocks forms the basis of our knowledge of past environments and life. The fraction of time preserved, however, is vanishingly small, which could indicate that preserved strata preferentially record the catastrophic and extreme events of the geologic past. Contrary to this expectation, field evidence across a range of scales suggests that fluvial strata predominantly record the mundane and relatively common transport conditions—a paradox termed the *strange ordinarieness* of fluvial strata. Using a new probabilistic modeling framework and existing experimental and field data, we suggest that the strange ordinarieness of fluvial strata is a result of the propensity of rivers to organize themselves into hierarchical elements (e.g., river dunes, bars, channels, and channel belts) that each have their representative timescale of evolution. We show that the presence of this hierarchy reconciles the paradox between the rarity of event preservation and the familiarity of the preserved events in stratigraphy at all scales. We also find that when successive hierarchical elements evolve at comparable rates, ordinary events are more likely to be preserved in stratigraphy. The story written in rocks is thus mostly of the common and mundane, not the rare and spectacular.

## 1. Introduction

Fluvial strata contain an archive of ancient environmental conditions and processes. However, active depositional time recorded in fluvial strata is vanishingly small (Ager & Trumpy, 1994; Dott, 1983; Plotnick, 1986; Sadler, 1981). This stratigraphic incompleteness is a result of geomorphic stasis and erosional hiatuses (Ganti et al., 2011; Paola et al., 2018; Straub & Foreman, 2018; Tipper, 2015) and might be thought to imply that the recorded events must be unusual and extreme in their magnitude and frequency (Ager, 1993a, 1993b), that is, the largest floods produce the deepest scours, which are preferentially preserved. Field observations across a range of scales, however, suggest the contrary: that fluvial deposition mostly occurs under fairly ordinary transport conditions (e.g., Armstrong et al., 2014; Ganti, Lamb, & McElroy, 2014; Hajek & Straub, 2017; Jerolmack & Paola, 2010; Paola, 2016; Paola et al., 2018; Reesink et al., 2015). Paola et al. (2018) termed this paradox between the rarity of event preservation and the quotidian nature of the preserved events the *strange ordinarieness* of fluvial strata. To understand this paradox, here we build on progress in understanding how time is recorded in strata (Paola et al., 2018; Sadler, 1981; Schumer & Jerolmack, 2009; Straub & Foreman, 2018; Tipper, 2015) to propose a theory for what controls the statistics of preserved *events* in fluvial strata.

Paola et al. (2018) suggest that the abundance of ordinary events—high frequency, low-to-moderate magnitude conditions that typify modern geomorphic observations—recorded in fluvial strata can result from the morphodynamic hierarchy of fluvial processes that span a multitude of scales (Figures 1a and 1b; Allen, 1966; Holbrook & Miall, 2020; Jackson, 1975; Miall, 2015). At a low level in the morphodynamic hierarchy, the relief of ripples and dunes is a fraction of the bankfull flow depth,  $H_{bf}$  (Bradley & Venditti, 2017; Yalin, 1964), and their migration timescales span minutes to days (Hajek & Straub, 2017). Similarly,  $H_{bf}$  determines the topographic relief of channel bars (Mohrig et al., 2000), with migration timescales that span days to decades (Hajek & Straub, 2017). At longer timescales, riverbeds aggrade relative to their surrounding floodplains; when this topographic relief reaches a small multiple of  $H_{bf}$  (Mohrig et al., 2000; Slingerland & Smith, 2004), channels relocate—avulse—with recurrence times ranging from decades to millennia (Edmonds et al., 2016; Ganti, Chu, et al., 2014; Jerolmack & Mohrig, 2007). On basin-filling timescales, the interplay among sediment supply, subsidence, and sea level changes determines the topographic evolution of fluvial systems (e.g., Paola, 2000); the maximum scale of variability at this level depends on the base level changes. For example, the magnitude of relative sea level changes over the last ~1 Ma spanned 3 to  $10H_{bf}$  for lowland rivers (Ganti, Lamb, & Chadwick, 2019; Li et al., 2016; Yu et al., 2017) and occurred on millennial to orbital timescales, causing regradation of the depositional surface (Hajek & Straub, 2017). Together, these observations suggest that morphodynamic hierarchical elements inherent in fluvial systems span 0.1 to  $10H_{bf}$  in their topographic relief, and their evolution occurs over minutes to millennia (Allen, 1966; Jackson, 1975; Miall, 2015). While the boundaries between the spatiotemporal scales of specific hierarchical elements are fuzzy (Figure 1a), each hierarchical element produces a distinct suite of depositional products identifiable in strata (e.g., Holbrook & Miall, 2020; Miall, 2015), including dune-scale cross-stratification, lateral accretion sets, channel bodies, and incised-valley fills.

Temporal changes in flow and sediment transport can further accentuate inherent scales of morphodynamic hierarchy. Abrupt flood recession can cause the abandonment of the relict, peak-flood-equilibrated dunes and bars that are cannibalized later by smaller, superimposed bedforms (Jones, 1977; Martin & Jerolmack, 2013; Myrow et al., 2018). Thus, natural discharge variability leads to the coexistence of bedforms of different scales (Allen, 1973; Myrow et al., 2018), and this type of hierarchical bedform organization may be prevalent in rivers (Leary & Ganti, 2020).

Our understanding of how fluvial morphodynamic hierarchy influences stratigraphic preservation is limited by the scales of observation possible in modern systems and in ancient strata and because physical experiments seldom resolve multiple, simultaneously active hierarchical elements. Here, we use a probabilistic framework to explore the role that the scales and rates of evolution of morphodynamic hierarchical elements play in the preservation of events in strata and validate our model results with existing experimental and field data that span similar hierarchical scales.

## 2. Material and Methods

### 2.1. Probabilistic Model of Fluvial Morphodynamic Hierarchy

Probabilistic investigation of physical stratigraphy dates back to the seminal work of Kolmogorov (1951) and has since provided key insights into the preservation of time and process in fluvial strata (Chamberlin & Hajek, 2015; Ganti et al., 2011; Schumer et al., 2011; Schumer & Jerolmack, 2009; Straub et al., 2012). Here we adopt a dimensionless vertical scale that hosts topographic variability organized into  $N$  hierarchical levels. We normalize the topographic relief of each level by  $H_{bf}$ —the fundamental vertical scale of a fluvial system. We represent the variability of the normalized topographic relief within each level using a two-parameter Gamma distribution with a shape parameter of 5 (Figure 1c and supporting information Text S1), consistent with observations of dunes and bars (Figure S1; Paola & Borgman, 1991). We use a maximum of  $N = 4$  levels (conceptually representing dunes, bars, channel-belts, and basin-scale topography), with dimensionless means of topographic relief of 0.25, 1, 3, and 8 (Figures 1a and 1c). While fluvial morphodynamic hierarchical elements are not limited to these classes alone, the vertical scales of topographic change span the entire spectrum expected in natural environments (Hajek & Straub, 2017; Holbrook & Miall, 2020; Miall, 2015).

We generated topographic sequences of individual levels,  $i$ , by equating the difference between the successive elevation maxima and minima to a random number generated from the  $i^{\text{th}}$  level Gamma distribution

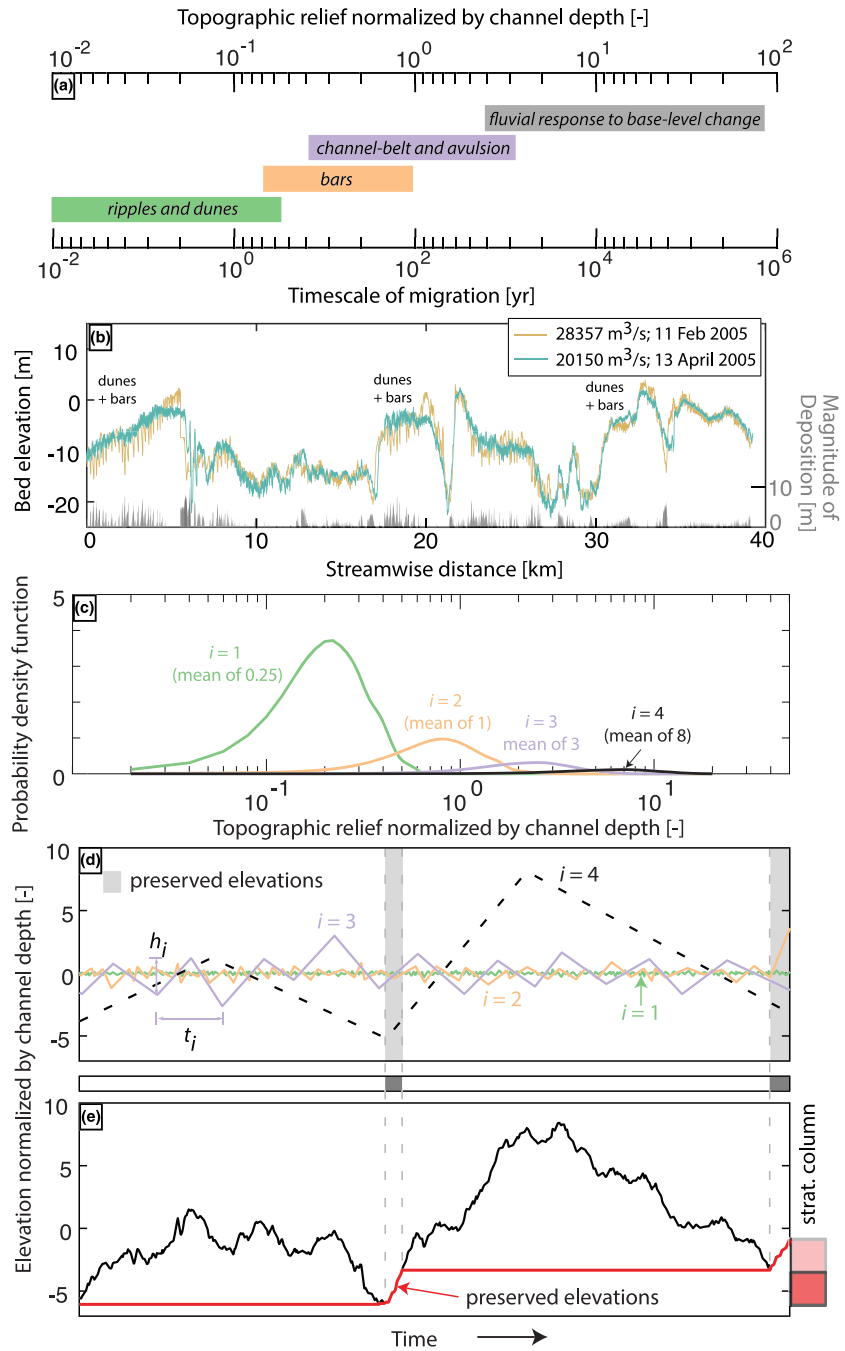


**Figure 1.** (a) Representative scales of fluvial morphodynamic hierarchy (after Hajek & Straub, 2017). (b) Successive 40-km-long profiles of the Lower Mississippi River (Leclair, 2011) highlight the hierarchical spatial organization prevalent in rivers. The gray bars denote the magnitude of deposition (right y axis) during the 8-week period, and zeros denote erosional reworking of deposits. (c) Two-parameter Gamma distributions of normalized topographic relief for different morphodynamic hierarchical levels. (d) Example topographic sequences from individual hierarchical levels with  $T_2 / T_1 = 5$ ,  $T_3 / T_1 = 50$ , and  $T_4 / T_1 = 100$ . The sum of these topographic sequences from hierarchical levels  $i = 1$  to  $N$  yields an independent realization of the normalized elevation time series with  $N = 4$  (black line), shown in (e). The red line indicates the synthetic stratigraphic elevation. The stratigraphic column is shown to the right, with the solid line indicating a bounding surface. The shaded gray area highlights the preserved elevations of individual elements.

(Figures 1c and 1d). The migration timescale of the elements comprising each hierarchical level  $i$  determines the distance between successive maxima and minima, which we equate to a uniformly distributed random variable with a mean of  $T_i$  (Figure 1d). Thus, the migration timescales of individual hierarchical elements vary across a predefined range. We set  $T_1 = 5$  [ $T_{1\min} = 1$  and  $T_{1\max} = 9$ ], and we systematically vary  $T_i / T_1$  for  $i > 1$  to explore its effect. After the spacing between the successive maxima and minima is determined, we linearly interpolate the elevations between these values (Figure 1d). Finally, we sum the topographic sequences over hierarchical levels  $i = 1, 2, \dots, N$ , where  $N$  is the highest-order level (Figure 1e). In our model, the migration timescale ( $T_i$ ) determines the kinematic rate of evolution within a hierarchical level, which conceptually captures the rate of bedform evolution ( $i = 1$ ), channel and bar migration ( $i = 2$ ), and channel-belt avulsion ( $i = 3$ ) in a fluvial network.

For each independent topographic realization (Figure 1e), we construct a synthetic stratigraphic column by removing deposited sediment that was subsequently eroded (e.g., Pelletier & Turcotte, 1997; Straub et al., 2012). We then track the original percentiles of preserved elevations arising from different levels (Figures 1d and 1e), denoted by  $p_{i,N}$ . For example,  $p_{1,1}$  and  $p_{1,4}$  denote the original percentiles of preserved elevations of the shortest-wavelength topography in the absence of morphodynamic hierarchy and when four hierarchical levels are present, respectively. We quantify the ordinarity of stratigraphy using a preserved extremality index,  $\Omega$ , defined as

$$\Omega = \frac{100 - 2\widetilde{p}_{i,N}}{100}, \quad (1)$$

where the tilde operator denotes the median. When extreme topographic lows (the deepest scours, i.e., low frequency, high magnitude conditions) dominate the preserved elevations, then  $\Omega \rightarrow 1$ ; conversely,  $\Omega \rightarrow 0$  indicates that preserved topography comes from more medial values in the body of the distribution and so is more “ordinary”.

We investigated the controls on the preservation for each hierarchical level,  $i$ , as a function of the total number of levels present ( $N$ ) and the relative timescales of migration of successive levels ( $T_{i+1} / T_i$ ). We also analyzed how net drift, which is akin to long-term sedimentation in a basin, affected  $\Omega$  at each hierarchical level. We report model results for 1,000 independent topographic realizations for each set of parameter values.

## 2.2. River Dune Experiments

We analyzed river dune evolution from two independent experiments by Ganti et al. (2013) and Martin and Jerolmack (2013). Both experiments were conducted in the tilting flume at St. Anthony Falls Laboratory, University of Minnesota (Text S2). We analyzed the “fast” flood experiment of Martin and Jerolmack (2013) and contrasted it with the steady-state experiment of Ganti et al. (2013). The steady-state experiment had a constant water discharge of  $0.08 \text{ m}^3/\text{s}$  for 20 hr, with no morphodynamic hierarchy present (Figure S5). In contrast, in the unsteady experiment, water discharge gradually increased from  $0.04$  to  $0.115 \text{ m}^3/\text{s}$  and back down to  $0.04 \text{ m}^3/\text{s}$  over 2 hr (Text S2; Martin & Jerolmack, 2013). This abrupt flood recession resulted in the coexistence of peak-flood-equilibrated dunes and smaller, superimposed dunes equilibrated with lower discharge (i.e., presence of morphodynamic hierarchy) during the flood recession and beyond (Figure S5). For both experiments, we constructed synthetic stratigraphic sections along a longitudinal transect and evaluated the preserved extremality index.

## 2.3. Field Data: Lower Mississippi River

We analyzed two 40-km-long profiles of the Lower Mississippi River collected during the falling limb of the spring flood of 2005, which were surveyed 8 weeks apart (Figure 1b; Leclair, 2011). Field observations highlight the coevolution of dunes and bars and the adjustment of dune topography to flow recession (Figure 1b). We constructed synthetic stratigraphy from these topographic surveys and tracked the preserved elevations. For consistency with our model, we used a piecewise linear function to remove the trend caused by the bar topography and then evaluated  $\Omega$  of dune topography (Text S3 and Figure S7). While the time span of the data is short compared to the timescales of preservation, this early preservation is an essential indicator of the eventual nature of stratigraphy.

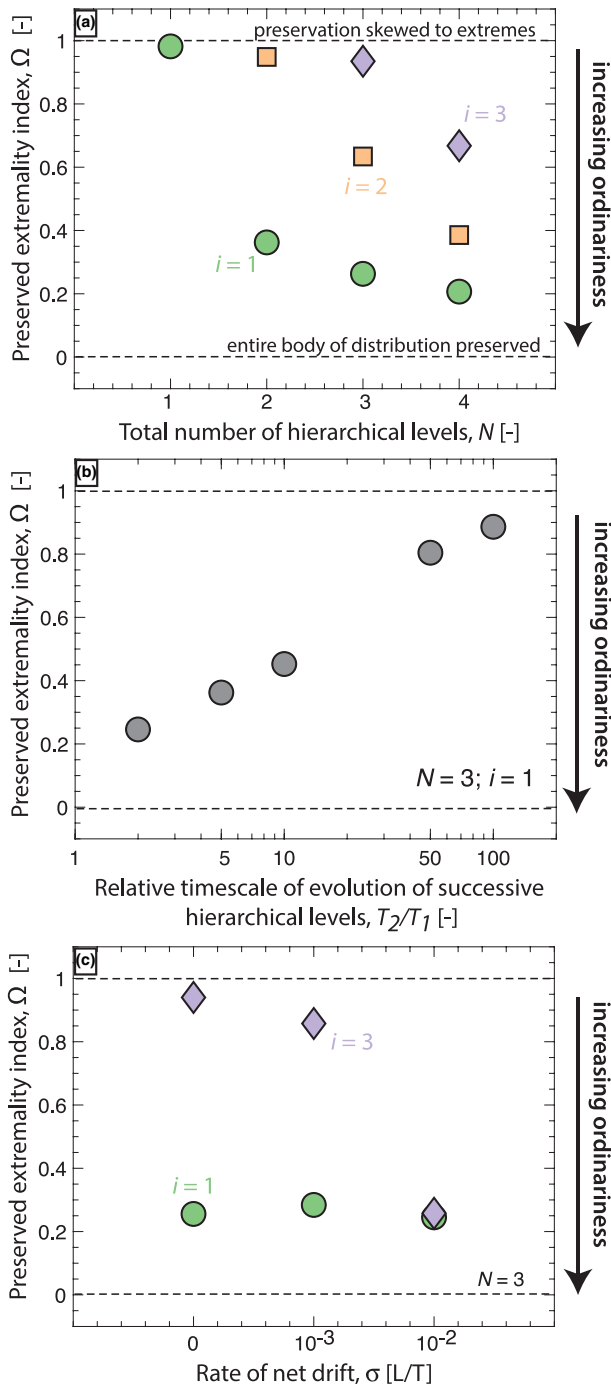


**Figure 2.** Functional dependence of the preserved extremality index ( $\Omega$ ; Equation 1) on (a) the total number of morphodynamic hierarchical levels for  $i = 1$  (circle), 2 (square), and 3 (diamond), (b) the relative timescale of evolution of successive hierarchical levels ( $T_2 / T_1$ ) for  $i = 1$  with  $N = 3$ , and (c) varying rates of net drift for the shortest-wavelength (circle) and longest-wavelength (diamond) topography with  $N = 3$ .

## 2.4. River Delta Experiments

To test the influence of relative rates of evolution of successive hierarchical levels on stratigraphic preservation, we compared two delta experiments that resolve the kinematics of channel migration ( $i = 2$  level) and avulsion ( $i = 3$  level). We analyzed a delta experiment conducted at the Caltech Earth Surface Dynamics laboratory (Ganti, Chadwick, Hassenruck-Gudipati, Fuller, & Lamb, 2016; Ganti, Chadwick, Hassenruck-Gudipati, & Lamb, 2016) and compared it with an experiment from the Tulane Delta Basin (Li et al., 2016, 2017; Straub et al., 2015). We term these experiments the *cohesionless experiment* and *cohesive experiment*. The cohesionless experiment had a constant base level, cohesionless sediment, subcritical flows, and variable water discharge such that the channels had high migration rates relative to their avulsion rates (high  $T_3 / T_2$ ; Text S4). The cohesive experiment had a constant infeed of sediment and water discharge, a steady base-level rise rate, and strongly cohesive sediment that resulted in channel migration rates more commensurate with avulsion rates (low  $T_3 / T_2$ ). We constructed the synthetic stratigraphy at one strike-oriented section for both the experiments and evaluated  $\Omega$  (Text S4).

## 3. Results

### 3.1. Model Results

In the absence of morphodynamic hierarchy ( $N = 1$ ), only the extreme elevations of the shortest-wavelength topography are preserved; the preserved extremality index is 0.92 (Figure 2a). We then systematically increased the total number of hierarchical levels from  $N = 2$  to 4 with  $T_2 / T_1 = 5$ ,  $T_3 / T_1 = 50$ , and  $T_4 / T_1 = 100$ . The order-of-magnitude difference between the successive  $T_i$  is representative of natural rivers, although this disparity could be larger (Hajek & Straub, 2017; Miall, 2015).

Increasing the number of levels increases the stratigraphic preservation of the shortest-wavelength topography, where their preserved elevations effectively spanned the entire formative distributions (Figures 2a, S2, and S3). For level 1,  $\Omega$  was 0.40, 0.28, and 0.22 for  $N = 2, 3$ , and 4, respectively. The enhanced preservation of topography was not limited to the shortest wavelength: the preservation of the  $i^{\text{th}}$  level was enhanced by the presence of an  $(i + 1)^{\text{th}}$  level at all scales (Figure 2a). In contrast, the preserved elevations from the highest level are derived from the extreme lows of the formative distribution ( $i = N$ ; Figures 2a and S2). For example, for  $i = 2$ ,  $\Omega$  was 0.95 when  $N = 2$  (Figure 2a).

The relative evolution timescales of successive hierarchical levels also have a profound influence on stratigraphic preservation. We evaluated  $\Omega$  for the shortest-wavelength topography for  $T_2 / T_1 = 2, 5, 10, 50$ , and 100, with  $N = 3$  (Figure 2b). For  $T_2 / T_1$  values of 2, 5, and 10, the preserved elevations from this shortest-wavelength topography effectively spanned their formative distribution, with  $\Omega = 0.24, 0.40$ , and 0.48, respectively (Figures 2b and S2). In contrast, for  $T_2 / T_1$  values of 50 and 100,  $\Omega$  increased to 0.74 and 0.84, respectively (Figure 2b). This result was consistent across levels, that is, values of  $T_{i+1} / T_i$  closer to unity reduced the preserved extremality index of the  $i^{\text{th}}$  level elevations (Figure S4). Finally, we found that the addition of net drift significantly improved the preservation of the more medial elevations only for the highest level ( $i = N$ ) and had a minimal effect on all lower-order levels (Figures 2c and S2).

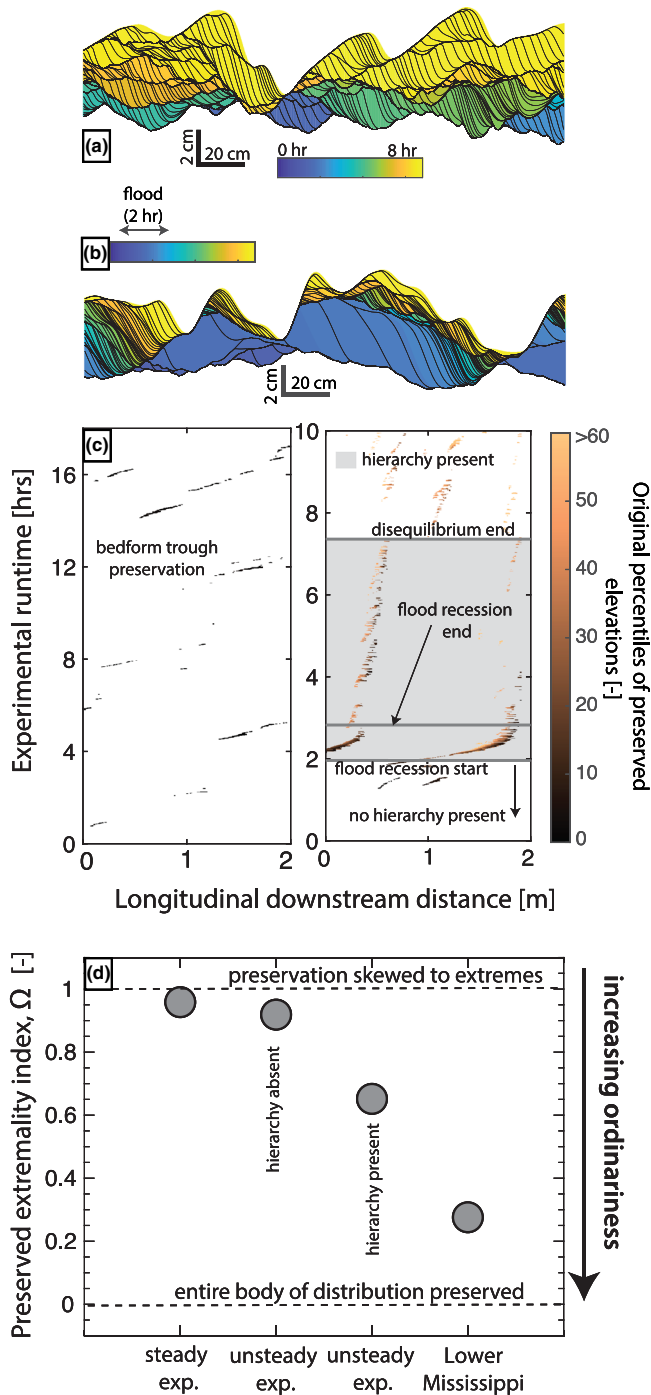


**Figure 3.** Synthetic stratigraphic sections, color-coded by experimental runtime, along a 2-m longitudinal transect for the (a) steady-state and (b) unsteady experiment. (c) Space-time matrix of preservation, color-coded by the original percentiles of preserved elevations, for the steady (left) and unsteady experiments (right). White and gray backgrounds denote no preservation and the presence of morphodynamic hierarchy, respectively. (d) Comparison of the preserved extremality index across the steady-state experiment, unsteady experiment with and without morphodynamic hierarchy, and the Lower Mississippi River.

### 3.2. Preservation at Dune Scale

For the steady-state experiment, only the bedform troughs were preserved, and preservation was spatiotemporally scattered (Figures 3a and 3c). The  $\Omega$  value was 0.96 (Figure 3d), consistent with our model results with  $i = 1$  and  $N = 1$  (Figure 2a). In contrast, preservation in the unsteady experiment was temporally concentrated in the flood recession when morphodynamic hierarchy developed owing to the lag between the bedform adjustment and the evolution of the flood wave (Figures 3b, 3c, and S5; Leary & Ganti, 2020). During this time, a larger fraction of the bedforms were preserved, compared to the steady-state experiment (Leary & Ganti, 2020):  $\Omega = 0.65$  for the disequilibrium phase of the unsteady experiment (Figure 3d). In contrast,  $\Omega = 0.92$  for the unsteady experiment—for other times, when the morphodynamic hierarchy was absent (Figure 3d).

For the Lower Mississippi data, the original percentiles of the preserved dune elevations spanned their entire formative distribution, with  $\Omega = 0.28$  (Figure 3d)—a value consistent with our model results for  $N > 1$  (Figure 2a).

### 3.3. Preservation at Basin-Filling Scales

In the cohesionless delta experiment, stratigraphic preservation was sparse, and only the channel troughs are preserved (Figures 4a and 4c). The high relative channel-migration rates resulted in channel bodies of high width-to-depth ratios (Figures 4a and 4c; Ganti, Lamb, et al., 2019), compared to the cohesive delta experimental deposits. The  $\Omega$  value for the cohesionless experiment was 0.74 (Figures 4e and S8), consistent with our model results with an order-of-magnitude difference between  $T_{i+1}$  and  $T_i$  (Figures 2b and S4). In contrast, the stratigraphic preservation was high in the cohesive experiment, with the positive relief of channels preserved in stratigraphy (Figures 4b and 4d). The  $\Omega$  value was 0.16 (Figures 4e and S8), consistent with our model results with comparable timescales of  $T_{i+1}$  and  $T_i$  (Figure 2d).

## 4. Discussion

In the absence of morphodynamic hierarchy, our results show that the preserved stratal boundaries originate from the extreme lows of the formative topography (Figures 2 and 3c). This result corresponds to the variability-dominated preservation model for bedforms (Reesink et al., 2015), where deposits are repeatedly reworked by migrating topography and the preservation of sets depends on the scour-depth variability (Leclair & Bridge, 2001; Paola & Borgman, 1991). The experimental deposits of the steady flood are consistent with our model results for this case (Figure 2a), where, in the absence of morphodynamic hierarchy,  $\Omega \rightarrow 1$  (Figures 3d and S6).

Our results indicate that a more medial fraction of the original topography is preserved in the presence of morphodynamic hierarchy. This enhanced preservation occurs at every lower-order hierarchical level, that is,  $i \ll N$  (Figures 2a, S2, and S3). These results are consistent with field observations of complete dune preservation in the presence of bars (Reesink et al., 2015) and the complete preservation of bars in avulsion-dominated systems (Chamberlin & Hajek, 2019). The results support the notion that morphodynamic hierarchy creates local “hot

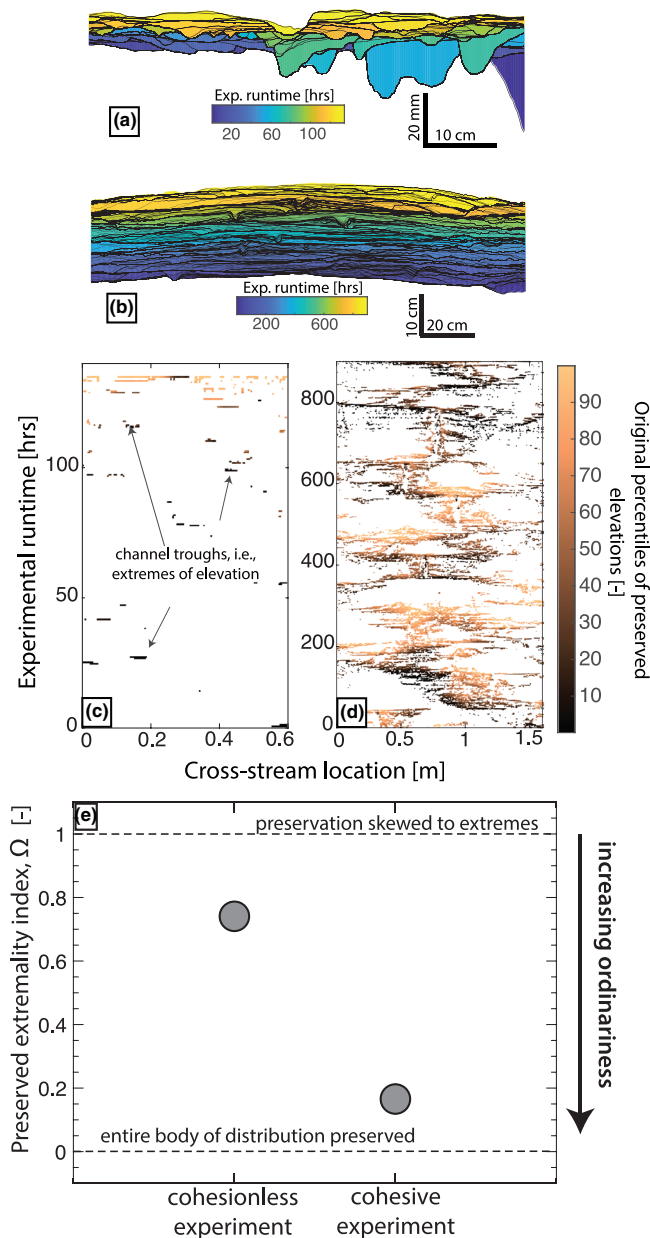


**Figure 4.** Strike-oriented synthetic stratigraphy and space-time matrices of preservation for the (a, c) cohesionless and (b, d) cohesive delta experiments. (e) Comparison of the preserved extremality index across the cohesionless and cohesive experiments.

spots” for preservation, where the higher-order hierarchical elements provide local accommodation for the preservation of lower-level elements via spatially focused high sedimentation (Leary & Ganti, 2020; Paola et al., 2018; Reesink et al., 2015).

At the bedform scale, the coexistence of relict, larger bedforms and smaller, superimposed bedforms, equilibrated with lower discharges, is characteristic of bedform disequilibrium (Myrow et al., 2018). This hierarchical spatial organization also causes enhanced sedimentation rates that likewise lead to preservation of a larger fraction of the formative topography—more medial or “ordinary” elevations—than expected under variability-dominated preservation (Leary & Ganti, 2020). Similarly, Reesink et al. (2015) argue that the enhanced preservation of dunes in the presence of bars is a result of the localized increase in sedimentation rates, consistent with our analysis of the Lower Mississippi data (Figures 1b and 3d). Together, these observations indicate that the existence of morphodynamic hierarchy in rivers—whether from inherent spatial self-organization or temporal discharge variability—results in the preservation of a broader range of the original bedform elevation distribution.

The relative evolution timescales of successive hierarchical levels play a significant role in stratigraphic preservation (Figure 2b). The ratio of the timescales of morphodynamic evolution of the  $(i + 1)^{\text{th}}$  and  $i^{\text{th}}$  levels determines the angle of climb for the lower-order elements (Figure 1d), with comparable values of  $T_{i + 1}$  and  $T_i$  resulting in a high angle of climb. Experimental results indicate that for systems dominated by lateral channel mobility (high  $T_3 / T_2$  owing to fast lateral migration rates; Figure 4), bar deposits are repeatedly reworked during the interavulsion period such that only a fraction of the bars is stratigraphically preserved (Chamberlin & Hajek, 2019). In contrast, in avulsion-dominated systems (low  $T_3 / T_2$  owing to slow lateral migration rates; Figure 4), bar deposits are minimally reworked in the interavulsion period resulting in high medial preservation (Figure 4; Chamberlin & Hajek, 2019). Additionally, our results indicate that net drift increases the medial preservation of only the highest-order level (Figure 2c), indicating that changes in long-term sedimentation rates should affect only the preservation statistics at the largest hierarchical scale (e.g., the compensation scale; Wang et al., 2011).

We highlight the utility of our framework in deciphering the causes of sedimentary architectural changes using two prominent examples. First, a unidirectional shift in fluvial strata is coincident with the radiation of embryophytes in the Silurian period (Davies & Gibling, 2010; Gibling & Davies, 2012). Postvegetation fluvial deposits are characterized by lateral accretion sets and a suite of width-to-depth ratios of channel-bodies; how-

ever, pre-Silurian river deposits exhibit high width-to-depth ratios (Cotter, 1977)—“sheet-braided” architecture—and truncated bar preservation (Davies & Gibling, 2010; Gibling & Davies, 2012). This stratigraphic shift is often associated with the rise of meandering rivers during the Silurian period, and pre-Silurian rivers are thought to be predominantly braided (e.g., Gibling et al., 2014; McMahon & Davies, 2018). Recent research, however, suggests that deeply channeled, single-threaded, pre-Silurian rivers were likely prevalent (Ielpi et al., 2017; Ganti, Whittaker, et al., 2019). Our results reconcile these apparent differences, suggesting that the observed architectural shift can arise from a reduction in the ratio of typical avulsion and channel-migration timescales ( $T_3 / T_2$  in our model; Figures 2b and 4e), instead of a singular change in river planform. This inference is bolstered by an order-of-magnitude decrease in channel migration rates ( $T_2$  in our model), forced by vegetation, in extant systems (Ielpi & Lapôtre, 2020).

As a second example, owing to changes in floodplain vegetation, flood variability, and climate-driven sediment supply (McInerney & Wing, 2011), rivers during the Paleocene-Eocene Thermal Maximum (PETM) are hypothesized to have high mobility (Foreman, 2014; Foreman et al., 2012). This increase in mobility for syn-PETM rivers can alter the relative evolution timescales of different levels in the morphodynamic hierarchy, compared to pre- and post-PETM rivers, and change the degree of preservation of dune, bar, and channel deposits (Figures 2b and 4). Our model results suggest that a preferential increase in avulsion rates driven by higher sediment flux should lead to the enhanced preservation of bar deposits in syn-PETM strata ( $\Omega \rightarrow 0$ ), compared to pre- and post-PETM deposits. However, if higher sediment supply simultaneously increased avulsion and channel-migration rates, then the preserved extremality index of bars will be consistent across the Paleocene and Eocene strata. Thus, careful mapping of apparent preservation of hierarchical elements should provide insights into the relative rates of morphodynamic processes on ancient landscapes (Chamberlin & Hajek, 2019; Greenberg, 2017).

Ultimately, sediment supply controls the rates of evolution of dunes, bars, and channel belts (Bryant et al., 1995; Constantine et al., 2014; Mahon & McElroy, 2018). These individual hierarchical elements, however, do not evolve in isolation, and the partitioning of sediment supply into bed-material transport, channel migration, and avulsion can have a profound influence on the physical fabric of the sedimentary record (Figure 2). Quantifying the hierarchical preservation of fluvial deposits provides a new technique to constrain their rates of evolution, relative to the next higher-order level, and help link estimates of paleo-sediment supply across scales. Moreover, while our model was developed for fluvial strata, it can be readily extended to other environments. For example, deepwater systems, crafted by turbidity currents, exhibit hierarchical organization into dunes, bars, channels, and channel belts (Wynn et al., 2007). While important differences exist between channelized systems in deepwater and terrestrial environments (Jobe et al., 2016, 2020; Wynn et al., 2007), our results suggest that stratigraphic preservation in deepwater environments is also likely controlled by the relative scales and rates of evolution of successive levels in the morphodynamic hierarchy.

## 5. Conclusions

Using a probabilistic model, coupled with experimental and field data, we show that the propensity of fluvial systems to self-organize into a morphodynamic hierarchy explains how ordinary transport conditions are routinely preserved in fluvial strata despite the vanishingly small overall preservation of elapsed time. We find that

1. Preserved stratal boundaries reflect extreme elevations (e.g., the deepest scours) only in the absence of the morphodynamic hierarchy;
2. Presence of morphodynamic hierarchy in a fluvial network increases the preservation of medial topography in all lower-order hierarchical elements;
3. Relative preservation of topography from a given morphodynamic level is highest when its evolution timescale is comparable to that of the next highest level; and
4. The preserved extremality index could provide new constraints on relative kinematic rates between successive levels in a morphodynamic hierarchy.

## Data Availability Statement

New experimental and field data were not generated in this study, and data for this study are from Leclair (2011), Ganti et al. (2013), Ganti, Chadwick, Hassenruck-Gudipati, Fuller, and Lamb (2016), Martin and Jerolmack (2013), and Straub et al. (2015).

## Acknowledgments

We thank Woodward Fischer for useful discussions and Rob Duller and an anonymous reviewer for constructive reviews. This work was supported by a National Science Foundation grant to Ganti (EAR 1935669) and Hajek (EAR 1935513) and by the donors of the American Chemical Society Petroleum Research Fund to Ganti.

## References

- Ager, D. V. (1993a). *The new catastrophism: The importance of the rare event in geological history*. Cambridge: Cambridge University Press.
- Ager, D. V. (1993b). *The nature of the stratigraphical record*. New York: John Wiley.
- Ager, D. V., & Trumpy, R. (1994). The nature of the stratigraphic record. *Sedimentary Geology*, 88(3-4), 315–316. [https://doi.org/10.1016/0037-0738\(94\)90075-2](https://doi.org/10.1016/0037-0738(94)90075-2)
- Allen, J. R. L. (1966). On bed forms and paleocurrents. *Sedimentology*, 6(3), 153–190. <https://doi.org/10.1111/j.1365-3091.1966.tb01576.x>
- Allen, J. R. L. (1973). Phase differences between bed configuration and flow in natural environments, and their geologic relevance. *Sedimentology*, 20(2), 323–329. <https://doi.org/10.1111/j.1365-3091.1973.tb02054.x>



- Armstrong, C., Mohrig, D., Hess, T., George, T., & Straub, K. M. (2014). Influence of growth faults on coastal fluvial systems: Examples from the late Miocene to Recent Mississippi River Delta. *Sedimentary Geology*, 301, 120–132. <https://doi.org/10.1016/j.sedgeo.2013.06.010>
- Bradley, R. W., & Venditti, J. G. (2017). Reevaluating dune scaling relations. *Earth-Science Reviews*, 165, 356–376. <https://doi.org/10.1016/j.earscirev.2016.11.004>
- Bryant, M., Falk, P., & Paola, C. (1995). Experimental study of avulsion frequency and rate of deposition. *Geology*, 23(4), 365–368. [https://doi.org/10.1130/0091-7613\(1995\)023%3C0365:ESOFAFA%3E2.3.CO;2](https://doi.org/10.1130/0091-7613(1995)023%3C0365:ESOFAFA%3E2.3.CO;2)
- Chamberlin, E. P., & Hajek, E. A. (2015). Interpreting paleo-avulsion dynamics from multistory sand bodies. *Journal of Sedimentary Research*, 85(2), 82–94. <https://doi.org/10.2110/jsr.2015.09>
- Chamberlin, E. P., & Hajek, E. A. (2019). Using bar preservation to constrain reworking in channel-dominated fluvial stratigraphy. *Geology*, 47, 1–4.
- Constantine, J. A., Dunne, T., Ahmed, J., Legleiter, C., & Lazarus, E. D. (2014). Sediment supply as a driver of river meandering and floodplain evolution in the Amazon Basin. *Nature Geoscience*, 7(12), 899–903. <https://doi.org/10.1038/ngeo2282>
- Cotter, E. (1977). The evolution of fluvial style, with special reference to the central Appalachian Paleozoic. *Fluvial Sedimentology*, 5, 361–383.
- Davies, N. S., & Gibling, M. R. (2010). Paleozoic vegetation and the Siluro-Devonian rise of fluvial lateral accretion sets. *Geology*, 38(1), 51–54. <https://doi.org/10.1130/G30443.1>
- Dott, R. H. (1983). Episodic sedimentation; how normal is average? How rare is rare? Does it matter? *Journal of Sedimentary Research*, 53(1), 5–23. <https://doi.org/10.1306/212F8148-2B24-11D7-8648000102C1865D>
- Edmonds, D. A., Hajek, E. A., Downton, N., & Bryk, A. B. (2016). Avulsion flow-path selection on rivers in foreland basins. *Geology*, 44(9), 695–698. <https://doi.org/10.1130/G38082.1>
- Foreman, B. Z. (2014). Climate-driven generation of a fluvial sheet sand body at the Paleocene-Eocene boundary in north-west Wyoming (USA). *Basin Research*, 26(2), 225–241. <https://doi.org/10.1111/bre.12027>
- Foreman, B. Z., Heller, P. L., & Clementz, M. T. (2012). Fluvial response to abrupt global warming at the Palaeocene/Eocene boundary. *Nature*, 491(7422), 92–95. <https://doi.org/10.1038/nature11513>
- Ganti, V., Chadwick, A. J., Hassenruck-Gudipati, H. J., Fuller, B. M., & Lamb, M. P. (2016). Experimental river delta size set by multiple floods and backwater hydrodynamics. *Science Advances*, 2(5), e150168. <https://doi.org/10.1126/sciadv.1501768>
- Ganti, V., Chadwick, A. J., Hassenruck-Gudipati, H. J., & Lamb, M. P. (2016). Avulsion cycles and their stratigraphic signature on an experimental backwater-controlled delta. *Journal of Geophysical Research: Earth Surface*, 121, 1651–1675. <https://doi.org/10.1002/2016JF003915>
- Ganti, V., Chu, Z., Lamb, M. P., Nittrouer, J. A., & Parker, G. (2014). Testing morphodynamic controls on the location and frequency of river avulsions on fans versus deltas: Huanghe (Yellow River), China. *Geophysical Research Letters*, 41, 7882–7890. <https://doi.org/10.1002/2014GL061918>
- Ganti, V., Lamb, M. P., & Chadwick, A. J. (2019). Autogenic erosional surfaces in fluvio-deltaic stratigraphy from floods, avulsions, and backwater hydrodynamics. *Journal of Sedimentary Research*, 89(8), 815–832. <https://doi.org/10.2110/jsr.2019.40>
- Ganti, V., Lamb, M. P., & McElroy, B. (2014). Quantitative bounds on morphodynamics and implications for reading the sedimentary record. *Nature Communications*, 5, 1–7.
- Ganti, V., Paola, C., Fofoula-Georgiou, E., & Fofoula-Georgiou, E. (2013). Kinematic controls on the geometry of the preserved cross sets. *Journal of Geophysical Research: Earth Surface*, 118, 1296–1307. <https://doi.org/10.1002/jgrf.20094>
- Ganti, V., Straub, K. M., Fofoula-Georgiou, E., & Paola, C. (2011). Space-time dynamics of depositional systems: Experimental evidence and theoretical modeling of heavy-tailed statistics. *Journal of Geophysical Research*, 116, F02011. <https://doi.org/10.1029/2010JF001893>
- Ganti, V., Whittaker, A. C., Lamb, M. P., & Fischer, W. W. (2019). Low-gradient, single-threaded rivers prior to greening of the continents. *Proceedings of the National Academy of Sciences*, 116(24), 11,652–11,657.
- Gibling, M. R., & Davies, N. S. (2012). Palaeozoic landscapes shaped by plant evolution. *Nature Geoscience*, 5(2), 99–105. <https://doi.org/10.1038/ngeo1376>
- Gibling, M. R., Davies, N. S., Falcon-Lang, H. J., Bashforth, A. R., DiMichele, W. A., Rygel, M. C., & Ielpi, A. (2014). Palaeozoic co-evolution of rivers and vegetation: A synthesis of current knowledge. *Proceedings of the Geologists Association*, 125(5-6), 524–533. <https://doi.org/10.1016/j.pgeola.2013.12.003>
- Greenberg, E. B. (2017). *Reconstructing river mobility from ancient deposits: An example from the Willwood Formation (Bighorn Basin, WY) (Master's thesis)*. state college, PA: Pennsylvania State University. Retrieved from <https://etda.libraries.psu.edu/catalog/14592ejg5302>
- Hajek, E. A., & Straub, K. M. (2017). Autogenic sedimentation in clastic stratigraphy. *Annual Review of Earth and Planetary Sciences*, 45(1), 681–709. <https://doi.org/10.1146/annurev-earth-063016-015935>
- Holbrook, J., & Miall, A. D. (2020). Time in the rock: A field guide to interpreting past events and processes from a fragmentary siliciclastic archive. *Earth-Science Reviews*, 203, 103121. <https://doi.org/10.1016/j.earscirev.2020.103121>
- Ielpi, A., & Lapôtte, M. G. A. (2020). A tenfold slowdown in river meander migration driven by plant life. *Nature Geoscience*, 13(1), 82–86. <https://doi.org/10.1038/s41561-019-0491-7>
- Ielpi, A., Rainbird, R. H., Ventra, D., & Ghinassi, M. (2017). Morphometric convergence between Proterozoic and post-vegetation rivers. *Nature Communications*, 8(1), 15,250. <https://doi.org/10.1038/ncomms15250>
- Jackson, R. G. II (1975). Hierarchical attributes and a unifying model of bed forms composed of cohesionless material and produced by shearing flow. *GSA Bulletin*, 86(11), 1523–1533. [https://doi.org/10.1130/0016-7606\(1975\)86%3C1523:HAAAUM%3E2.0.CO;2](https://doi.org/10.1130/0016-7606(1975)86%3C1523:HAAAUM%3E2.0.CO;2)
- Jerolmack, D. J., & Mohrig, D. (2007). Conditions for branching in depositional rivers. *Geology*, 35(5), 463–466. <https://doi.org/10.1130/G23308A.1>
- Jerolmack, D. J., & Paola, C. (2010). Shredding of environmental signals by sediment transport. *Geophysical Research Letters*, 37, L19401. <https://doi.org/10.1029/2010GL044638>
- Jobe, Z. R., Howes, N. C., & Aucther, N. C. (2016). Comparing submarine and fluvial channel kinematics: Implications for stratigraphic architecture. *Geology*, 44(11), 931–934. <https://doi.org/10.1130/G38158.1>
- Jobe, Z. R., Howes, N. C., Straub, K. M., Cai, D., Deng, H., Laugier, F. J., et al. (2020). Comparing aggradation, superelevation, and avulsion frequency of submarine and fluvial channels. *Frontiers in Earth Science*, 8. <https://doi.org/10.3389/feart.2020.0053>
- Jones, C. M. (1977). Effects of varying discharge regimes on bed-form sedimentary structures in modern rivers. *Geology*, 5(9), 567–570. [https://doi.org/10.1130/0091-7613\(1977\)5%3C567:EOVDRO%3E2.0.CO;2](https://doi.org/10.1130/0091-7613(1977)5%3C567:EOVDRO%3E2.0.CO;2)
- Kolmogorov, A. N. (1951). Solution of a problem in probability theory connected with the problem of the mechanism of stratification. *American Mathematical Society Transactions*, 53, 171–177.

- Leary, K. C. P., & Ganti, V. (2020). Preserved fluvial cross strata record bedform disequilibrium dynamics. *Geophysical Research Letters*, *47*, e2019GL085910. <https://doi.org/10.1029/2019gl085910>
- Leclair, S. F. (2011). Interpreting fluvial hydromorphology from the rock record: Large-river peak flows leave no clear signature. *From river to rock Rec. Preserv. Fluv. sediments their Subseq. Interpret. SEPM Spec. Publ.*, *97*, 113–123.
- Leclair, S. F., & Bridge, J. S. (2001). Quantitative interpretation of sedimentary structures formed by river dunes. *Journal of Sedimentary Research*, *71*(5), 713–716. <https://doi.org/10.1306/2DC40962-0E47-11D7-8643000102C1865D>
- Li, Q., Matthew Benson, W., Harlan, M., Robichaux, P., Sha, X., Xu, K., & Straub, K. M. (2017). Influence of sediment cohesion on deltaic morphodynamics and stratigraphy over basin-filling time scales. *Journal of Geophysical Research: Earth Surface*, *122*, 1808–1826. <https://doi.org/10.1002/2017JF004216>
- Li, Q., Yu, L., & Straub, K. M. (2016). Storage thresholds for relative sea-level signals in the stratigraphic record. *Geology*, *44*(3), 179–182. <https://doi.org/10.1130/G37484.1>
- Mahon, R. C., & McElroy, B. (2018). Indirect estimation of bedload flux from modern sand-bed rivers and ancient fluvial strata. *Geology*, *46*(7), 579–582. <https://doi.org/10.1130/G40161.1>
- Martin, R. L., & Jerolmack, D. J. (2013). Origin of hysteresis in bed form response to unsteady flows. *Water Resources Research*, *49*, 1314–1333. <https://doi.org/10.1002/wrcr.20093>
- McInerney, F. A., & Wing, S. L. (2011). The Paleocene-Eocene thermal maximum: A perturbation of carbon cycle, climate, and biosphere with implications for the future. *Annual Review of Earth and Planetary Sciences*, *39*(1), 489–516. <https://doi.org/10.1146/annurev-earth-040610-133431>
- McMahon, W. J., & Davies, N. S. (2018). The shortage of geological evidence for pre-vegetation meandering rivers. *Fluvial Meanders and Their Sedimentary Products in the Rock Record*, 119–148. <https://doi.org/10.1002/9781119424437.ch5>
- Miall, A. D. (2015). Updating uniformitarianism: Stratigraphy as just a set of ‘frozen accidents’. *Geological Society of London, Special Publication*, *404*(1), 11–36. <https://doi.org/10.1144/SP404.4>
- Mohrig, D., Heller, P. L., & Lyons, W. J. (2000). Interpreting avulsion process from ancient alluvial sequences: Guadalupe-Matarranya system (northern Spain) and Wasatch Formation (western Colorado). *Geological Society of America Bulletin*, *112*(12), 1787–1803. [https://doi.org/10.1130/0016-7606\(2000\)112%3C1787:IAPFAA%3E2.0.CO;2](https://doi.org/10.1130/0016-7606(2000)112%3C1787:IAPFAA%3E2.0.CO;2)
- Myrow, P. M., Jerolmack, D. J., & Perron, J. T. (2018). Bedform disequilibrium. *Journal of Sedimentary Research*, *88*, 1096–1113.
- Paola, C. (2000). Quantitative models of sedimentary basin filling. *Sedimentology*, *47*, 121–178. <https://doi.org/10.1046/j.1365-3091.2000.00006.x>
- Paola, C. (2016). A mind of their own: Recent advances in autogenic dynamics in rivers and deltas. In D. A. Budd, E. A. Hajek, & S. J. Purkis (Eds.), *Autogenic dynamics and self-organization in sedimentary systems*, (pp. 5–17). Tulsa, Oklahoma: SEPM Society for Sedimentary Geology.
- Paola, C., & Borgman, L. (1991). Reconstructing random topography from preserved stratification. *Sedimentology*, *38*(4), 553–565. <https://doi.org/10.1111/j.1365-3091.1991.tb01008.x>
- Paola, C., Ganti, V., Mohrig, D., Runkel, A. C. and Straub, K.M. (2018) Time not our time: Physical controls on the preservation and measurement of geologic time. *Annual Review of Earth and Planetary Sciences.*, *46*, annurev-earth-082517-010129.
- Pelletier, J. D., & Turcotte, D. L. (1997). Synthetic stratigraphy with a stochastic diffusion model of fluvial sedimentation. *Journal of Sedimentary Research*, *67*, 1060–1067.
- Plotnick, R. E. (1986). A fractal model for the distribution of stratigraphic hiatuses. *Journal of Geology*, *94*(6), 885–890. <https://doi.org/10.1086/629094>
- Reesink, A. J. H. H., Van den Berg, J. H., Parsons, D. R., Amsler, M. L., Best, J. L., Hardy, R. J., et al. (2015). Extremes in dune preservation: Controls on the completeness of fluvial deposits. *Earth-Science Reviews*, *150*, 652–665. <https://doi.org/10.1016/j.earscirev.2015.09.008>
- Sadler, P. M. (1981). Sediment accumulation rates and the completeness of stratigraphic sections. *Journal of Geology*, *89*(5), 569–584. <https://doi.org/10.1086/628623>
- Schumer, R., Jerolmack, D., & McElroy, B. (2011). The stratigraphic filter and bias in measurement of geologic rates. *Geophysical Research Letters*, *38*, 1–4. <https://doi.org/10.1029/2011GL047118>
- Schumer, R., & Jerolmack, D. J. (2009). Real and apparent changes in sediment deposition rates through time. *Journal of Geophysical Research*, *114*, F00A06. <https://doi.org/10.1029/2009JF001266>
- Slingerland, R., & Smith, N. D. (2004). River avulsions and their deposits. *Annual Review of Earth and Planetary Sciences*, *32*(1), 257–285. <https://doi.org/10.1146/annurev-earth.32.101802.120201>
- Straub, K. M., & Foreman, B. Z. (2018). Geomorphic stasis and spatiotemporal scales of stratigraphic completeness. *Geology*, *46*(4), 311–314. <https://doi.org/10.1130/G40045.1>
- Straub, K. M., Ganti, V., Paola, C., & Foufoula-Georgiou, E. (2012). Prevalence of exponential bed thickness distributions in the stratigraphic record: Experiments and theory. *Journal of Geophysical Research*, *117*, F02003. <https://doi.org/10.1029/2011JF002034>
- Straub, K. M., Li, Q., & Benson, W. M. (2015). Influence of sediment cohesion on deltaic shoreline dynamics and bulk sediment retention: A laboratory study. *Geophysical Research Letters*, *42*, 9808–9815. <https://doi.org/10.1002/2015GL066131>
- Tipper, J. C. (2015). The importance of doing nothing: Stasis in sedimentation systems and its stratigraphic effects. *Geological Society of London, Special Publication*, *404*(1), 105–122. <https://doi.org/10.1144/SP404.6>
- Wang, Y., Straub, K. M., & Hajek, E. A. (2011). Scale-dependent compensational stacking: An estimate of autogenic time scales in channelized sedimentary deposits. *Geology*, *39*(9), 811–814. <https://doi.org/10.1130/G32068.1>
- Wynn, R. B., Cronin, B. T., & Peakall, J. (2007). Sinuous deep-water channels: Genesis, geometry and architecture. *Marine and Petroleum Geology*, *24*(6–9), 341–387. <https://doi.org/10.1016/j.marpetgeo.2007.06.001>
- Yalin, M. S. (1964). Geometrical properties of sand waves. *Journal of the Hydraulics Division*, *90*, 105–119.
- Yu, L., Li, Q., & Straub, K. M. (2017). Scaling the response of deltas to relative-sea-level cycles by autogenic space and time scales: A laboratory study. *Journal of Sedimentary Research*, *87*(8), 817–837. <https://doi.org/10.2110/jsr.2017.46>